Force measuring optical tweezers system for long time measurements of P pili stability

Magnus Andersson[a], Erik Fällman[a], Bernt Eric Uhlin[b] and Ove Axner[a*]

[a]Department of Physics, Umeå University, SE-901 87 Umeå, Sweden
[b]Department of Molecular Biology, Umeå University, SE-901 87 Umeå, Sweden

ABSTRACT

A force-measuring optical tweezers instrumentation and long time measurements of the elongation and retraction of bacterial fimbriae from Uropathogenic *E. coli* (UPEC) under strain are presented. The instrumentation is presented in some detail. Special emphasis is given to measures taken to reduce the influence of noise and drifts in the system and from the surrounding, which makes long term force measurements possible. Individual P pili from UPEC bacteria were used as a biological model system for repetitive unfolding and refolding cycles of bacterial fimbriae under equilibrium conditions. P pili have evolved into a three-dimensional helix-like structure, the PapA rod, that can be successively and significantly elongated and/or unfolded when exposed to external forces. The instrumentation is used for characterization of the force-*vs.*-elongation response of the PapA rod of individual P pili, with emphasis on the long time stability of the forced unfolding and refolding of the helical structure of the PapA rod. The results show that the PapA rod is capable of withstanding extensive strain, leading to a complete unfolding of the helical structure, repetitive times during the life cycle of a bacterium without any noticeable alteration of the mechanical properties of the P pili. This function is believed to be importance for UPEC bacteria in vivo since it provides a close contact to a host cell (which is an initial step of invasion) despite urine cleaning attempts.

Keywords: Force measuring optical tweezers, Bacterial fimbriae, *E. coli*, P pili, PapA, unfolding and refolding, Macromolecules

1. INTRODUCTION

Optical tweezers (OT) have, during the last decade, grown into a powerful tool for assessments of minute forces in the field of nanoscience in general and those in biology in particular.[1] The technique makes use of a bead trapped in the focus of a strong laser beam as the force transducer. If the bead is exposed to an external force, its position in the trap will shift. Correctly constructed, force measuring optical tweezers (FMOT) can provide absolute forces measurements in the 0.1 – 200 pN range, which is one order of magnitude better than the widely used atomic force microscopy (AFM) technique.[2] This makes FMOT the number one option when it comes to measurements of forces in the low pN regime.

Since many types of adhesion forces in biological systems, non-covalent bond strengths, and entropic forces in large chain-like biomolecules often are in the tens of pN range, FMOT is very suitable for assessments of weak interaction forces in biological systems.[3] Moreover, the FMOT technique can measure both static forces, for example stall forces of motor proteins, and dynamic properties of biomolecules and interactions, even those of a single bond.[4,5] A variety of investigations of forces created by single bonds, associated with folding of macromolecules, e.g. DNA, or adhesion, have therefore been performed during the last years.[3-6] These studies have revealed several new mechanical or biophysical properties of various biopolymers and given new insight into the behavior of biological macromolecules.

However, most measurements, in particular those based upon dynamic force spectroscopy (DFS), are made under a relatively short time (for a few seconds or a part thereof).[5] This implies that drifts in the instrumentation are not affecting the measurements to the same degree as when studies under equilibrium conditions or long terms

* Ove.axner@physics.umu.se; phone +46–90 786 6754; fax +46–90 786 6673; www.phys.umu.se/exphys/Laser_Physics_Group/

investigations are performed. Because of the 1/*f*-nature of low frequency drifts and noise, it is in fact substantially more difficult to perform an accurate assessment of the biophysical properties of a macromolecule or a biological system under long times (minutes or hours) than under the conditions for DFS. Long term studies require both a stable FMOT system and a stable measuring environment. Whereas the first can be achieved by well designed instrumentation, consisting of stable lasers, an optical system that is insensitive to minor fluctuations of the beam or vibrations, a stable microscope, low noise detectors and electronics, the latter calls for, among other things, non-fluctuating room and microscope temperatures, all of which contribute to low background noise and drifts. This work presents a FMOT system that can provide stable conditions for sensitive force measurements over long time and exemplifies this by long time measurements of the elongation of P pili from uropathogenic *E. coli* (UPEC) exposed to external forces.

In short, UPEC bacteria colonize the urinary tract and are implicated in 75-80% of uncomplicated urinary tract infections as well as in severe pyelonephritis (upper urinary tract and kidney infections).[7,8] They express various types of fimbrial adhesins, pili, which are responsible for mediating adhesion and maintaining bacteria-host contact during the initial stages of infections. Since the success of a bacterial infection often depends on the ability of the bacteria to resist the action of the surrounding environment – for UPEC the cleaning actions from the flow of urine that gives rise to shear forces – the structure of bacterial pili and their response to external forces are issues of importance.

P pili are a type of pili that predominantly are expressed by isolates from the upper urinary tract (they are expressed by approximately 90% of the E. coli strains that cause pyelonephritis).[7,8] They therefore constitute an important virulence factor.[9] They have evolved into a three-dimensional helix-like structure, the PapA rod,[10-14] that can be successively and significantly elongated and/or unfolded when exposed to external forces.[13-18] The PapA rod is a thin micrometer-long helical rod composed of ~103 subunits that are coupled to their nearest neighbors by a β-strand complementation and combined in a right handed helical arrangement with 3.28 units per turn.[11-14] It has been hypothesized that the structure of the P pili, with its flexible structure and intricate unfolding mechanism, makes it possible for a UPEC bacterium to withstand considerable shear forces by a process in which a large number of pili can support tension simultaneously, despite dissimilar bacterium-to-host distances,[13,14] which, in turn, could explain why they can remain attached to the host tissue even in the presence of considerable urine flows. This hypothesis has not yet been verified in vivo. On the other hand, various works have been performed throughout the years aiming for a characterization of P pili with regard to their structure as well as various biomechanical properties.†

Until recently, individual P pili had only been characterized with respect to their protein composition and static structure (their size and three-dimensional shape).[10-14] However, because of the specific importance and unique behavior of E. coli P pili, their intrinsic mechanical properties were recently assessed using FMOT, both under conventional (steady-state) and dynamic modes of operation.[15-18] It was found that the PapA rod possesses a rich flavor of elongation and contraction behavior. For example, in addition to initial elastic stretching, the elongation of a P pilus takes place by a sequential and cooperative unfolding of its PapA rod.[15,18] When the entire rod has become unfolded, it elongates further by an overstretching of the head-to-tail bond through a phase transition in a non-cooperative manner, strongly affected by entropy.[18] It has also been shown that the unfolding of the PapA rod is fully reversible under equilibrium conditions, which contradicts earlier predictions that the unfolding should be plastic.[13,16] Despite these studies, P pili have not yet been investigated with respect to its long-term properties, e.g. stability and unfolding/refolding, which are believed to be of importance for the infection ability of bacteria in vivo since it provides a close contact to a host cell despite repeated cleaning attempts, primarily due to the limited long-term stability of conventional FMOT systems. The FMOT system presented in this work is therefore used for measurements and assessments of long-term properties of P

† One of the largest threats to mankind of today is the antibiotic resistant bacteria strains that have resulted from the heavy use of antibiotics during the last decades. It is an irrefutable fact that new methods of combating infections are therefore urgently needed. One such approach is to address the bacteria's ability to invade tissue. Since target cell adhesion is the initial step of colonization, bacterial adhesion could be a possible aim for new drugs. In order to find means to address this issue, the adhesion behavior of bacteria needs to be characterized and targets for new drugs need to be identified. The characterization of P pili by optical tweezers that recently have been done[10-14] and currently is under way is a part of such an investigation.

pili from UPEC bacteria. The measurements demonstrate both the stability of the FMOT experimental setup and the long term reproducibility of the unfolding and refolding of the PapA rod.

2. MATERIALS AND METHOD

2.1. The optical tweezers system

The optical tweezers force measurement system was built on a vibration isolated (floating) optical table (TMC) around an inverted microscope (IX-71, Olympus) modified for introducing laser light both for trapping and position monitoring of a trapped object. The microscope, schematically illustrated in Fig. 1, was placed on top of a 5 mm thick layer of bakelite for temperature isolation.

A linear polarized diode pumped Nd:YAG laser (Millenia IR 10W, Spectra Physics), with a TEM00 mode, was used for trapping since this laser provides good beam quality with low amounts of intensity and pointing fluctuations and since cells have a fairly low absorption coefficient at the 1064 nm wavelength. The trapping light was fed into the microscope through a set of optics (consisting of four mirrors and three lenses) that shaped the beam to the correct size and divergence and provided a possibility for accurate adjustments of the trap in the sample. The laser was directed into the microscope by the use of an IR antireflection coated dichroic mirror (HR1064HT633 + 337/45/BBAR RW33-25.4-3UV, SWP-L.-M.33x1, Laser components GmbH) placed in the right side port of the microscope and was optimized so it was slightly overfilling the entrance pupil of a high numerical aperture objective (Olympus UPLFL100X/IR, NA 1.30). The optical system provides a steering of the trap in the lateral direction of the sample plane by a piezo controlled mirror (Model S226, Physik Instrumente) positioned at the image plane of the entrance pupil of the objective, whereas the axial movement can be controlled by changing the divergence of the beam via an afocal lens system, according to the recipe in Ref.[19]. This optical system provides adjustments of the trap in 3-D without any loss of power by a pivoting of the laser beam around the entrance pupil of the microscope objective. In addition to provide good moveability of the trap in the specimen plane, this recipe also reduces the influence of vibrations of the mirrors and lenses on the stability of the trap. To avoid laser light reflections to the eyes, a laser blocking filter (Hot mirror, 840, Omega Optical) was placed in front of the oculars. The laser was run at a power of ~1.0 W, which gave rise a stiffness of 1.4 10^{-4} N/m.

The displacement of the trapped bead from the equilibrium position is a direct measurement of the force in the system. A separate probe laser was used for monitoring the position of the bead in the trap since this has a number of advantages. One is that it can be separately adjusted for best detection conditions. Another is that a separate probe laser can have a smaller divergence that the trapping beam (which is achieved by underfilling the objective), which makes it possible to use a dry condenser instead of an oil condenser (which normally is used when high NA objectives are used) for illumination as well as focusing of the probe beam. A dry condenser is not only easier to use than an oil condenser (no oil and no disturbing air bubbles), it has also the advantage that it reduces vibrations by separating the condenser from the cover glass. Except for transferring vibrations from the microscope arm to the sample, an oil condenser has also the disadvantage that it can make it more difficult to keep a stable temperature since a sample of a few µL is strongly affected by its surrounding environment, in particular such a significant heat-sink as an oil condenser. Force measurements on biological systems under normal conditions, (e.g. 37º C and in an CO_2 environment) in a heated sample holder can therefore more easily be implemented if a dry condenser is used. A third advantage is that the probe laser can have a wavelength sufficiently dissimilar from the trapping laser so that an efficient separation of the probe and trapping laser light field can be done prior to the position sensitive detector, whereby an effect such as saturation of the detector can be avoided. The bandwidth limitation of silicon-based photodetectors due to low absorption of infrared light has been shown by Berg-Sorenson.[20]

The laser used for probing the position of the bead in the trap was an optical-fiber-coupled (SMJ-A3A, 3AF-633-4/125-3-1, OZ Optics LTD) linearly polarized HeNe laser (1137, Uniphase, Manteca). There are several advantages of using a fiber-coupled laser as a probe laser. First of all, it cleans the spatial mode of the beam, which improves both the focusing of the beam in the specimen plane and the imaging onto the detector. Secondly, it reduces the number of mirrors and lenses that needs to be used in the system. Since each mirror and lens can introduce noise in the system by

acting as antennas for vibrations, this reduces the amount of noise in the system. Thirdly, it is very stable over time and facilitates optimization since it is easy to adjust. Yet another advantage is that it is in general less expensive than the corresponding number of lenses, mirrors and holders.

Following the patent of Chu and Kron,[21] a fiber focuser (HPUFO-2, A3A-400/700-S-17-180-10AC, OZ Optics LTD) was mounted at the end of the fiber, which, in turn, was positioned on a xyz-micrometer stage for accurate alignment. The light was thereafter directed towards a Gimbal mounted mirror. The use of a micrometer stage in combination with a Gimbal mounted mirror made it possible to align the focus of the light in a very precise manner (in the x, y, z, θ, and φ directions). The probe laser light was then introduced into the microscope through a side port and directed towards the objective by the use of a polarizing beam splitter cube (PBSH-760-980-100; CVI laser Corporation). The focus of the light after the fiber focuser was positioned in close proximity of the image plane of the trapped bead in such a way that the beam focused slightly below the trapped bead in the specimen plane. The probe beam was then adjusted so that an as large linear detector-signal-*vs.*-bead-position region as possible was be obtained, since the absence of non-linearities in this response is considered to be a good indicator that the detection optics is properly aligned.

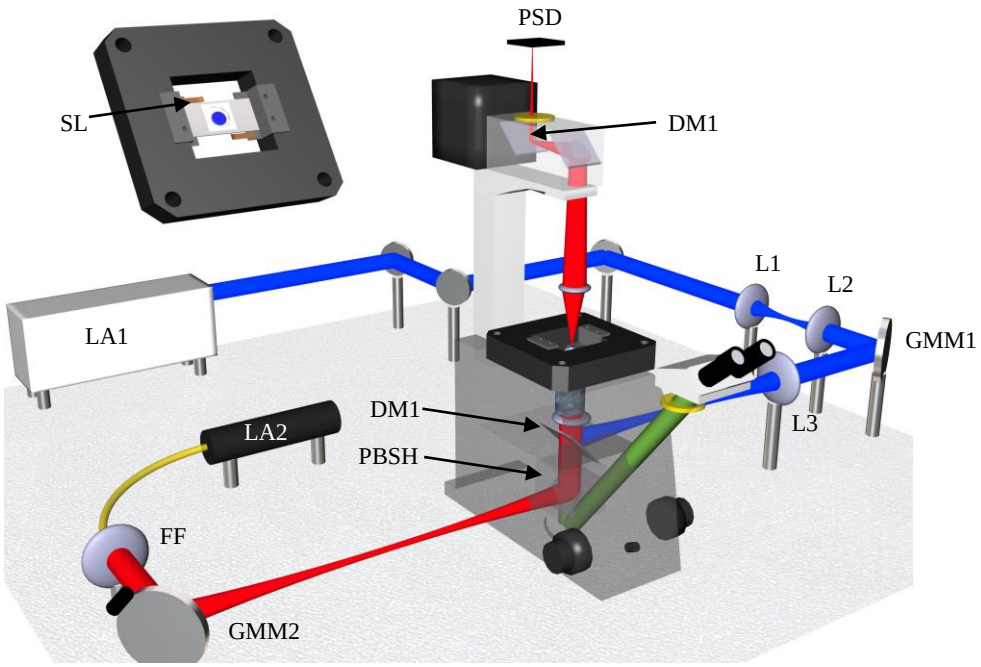

Figure 1. The layout shows the force measuring optical tweezers setup where the essential components are as follows. A cw Nd:YAG laser, LA1, is used for trapping, the trapping position in the z-direction is controlled via the lens, L1 (f = 60 mm, model no. LPX 125/083; Melles Griot), which together with L2 (f = 60 mm, model no. LPX 125/083; Melles Griot) forms an afocal lens system. A computer controlled gimbal mounted mirror, GMM1, controls the x-direction of the position of the trap in the sample plane. The entrance aperture of the objective is imaged onto the surface of the gimbal mounted mirror by a second afocal lens system, produced by an external lens L3, (f = 150 mm, model no. LPX 238/083; Melles Griot) and the tube lens inside the microscope. The light is introduced via a dichroic mirror, DM1, coated for reflecting 1064 nm light and with a high transmission for visible light. A fiber-coupled HeNe laser, LA2, with a fiber focuser, FF, reflected via a gimbal mounted mirror, GMM2, and introduced via a polarizing beam splitter cube, PBSH, is used for probing the position of the trapped object. The probe laser light is image via the microscope condenser and a second dichroic mirror, DM2, onto a position sensitive detector, PSD. The sample is placed on a custom made slide holder, SL, mounted in a piezo stage.

The power of the probe light was around 0.1 mW (measured at the entrance aperture of the objective). In order to reduce the influence of fluctuations of the probe laser (primarily intensity variations), the detection of the position of the

probe laser was made by the use of a position sensitive detector (PSD, model no. L20 SU9; Sitek Electro Optics, Sweden) from which an intensity normalized output signal was created as $(I_1 - I_2)/(I_1 + I_2)$, where I_1 and I_2 are the currents from the two outputs of the PSD, respectively. This reduced significantly noise and fluctuations in the detector signal that originate from intensity fluctuations.

An additional closed loop x,y-piezo stage (P517.2CL, Physik Instrumente) was mounted on top of the existing step motor stage for nm resolution positioning and steering. The piezo can be controlled via a computer interface for accurate movement, and the absolute position of the stage is sampled for computing the exact elongation distance. A home made slide holder was firmly attached on the piezo stage onto which a home-built sample cell, consisting of two cover slides separated by a 1 mm aluminum frame with a 1 cm hole in the middle, was secured. The bottom cover slide of the sample cell was securely fastened to the piezo stage with two clips on each side to prevent it from settling down during long-time measurements. A typical sample volume of 30 µL was prepared and placed on the bottom slide, where after a top slide is carefully place as a lid and firmly secured.

All mirrors and lenses in the optical system were placed in robust holders in order to minimize the amount of fluctuations they introduce through mechanical vibrations. The instrumentation was placed in a temperature controlled room with all noise generating equipment such as computers, controllers, and drivers placed outside. Remote controlled interfaces and automated computer programs make it possible, if needed, to perform measurements from the outside of the room to reduce human influence of the measurement. All procedures involving calibration, movements of piezo stage and mirrors, and finally the measuring process, were controlled by a custom made LabView program.

2.2. The calibration procedure

In order to measure absolute forces accurately it is of importance that the stiffness of the trap (for the particular bead used) is calibrated in a proper way. There are different ways of calibrating the trap stiffness,[22] of which the most suitable for our purposes is that based upon a power spectrum analysis of the fluctuations the bead makes in the trap due to the combined effects of thermal (Brownian) motion and the restoring force in the trap. A bead undergoing thermal motion in a harmonic potential (the trap) can be described by the Langevin function.[22] The power spectrum of such a movement, $S(f) = |X(f)|^2$, has a Lorentzian form and can be expressed as,

$$S(f) = \frac{k_B T}{\gamma \pi^2 (f^2 + f_c^2)}, \qquad (1)$$

where γ is the viscous drag coefficient, where f_c the corner frequency, related to the stiffness of the trap, κ, by $\kappa = 2\pi\gamma f_c$, and where $k_B T$ takes a numerical value of 4.1 pN nm at room temperature. The stiffness of the trap is then obtained from the corner frequency and the constant (low-frequency) level, $S(f \ll f_c)$, in a fit of Eq (1) to the sampled data.

A total of 2^{19} (524 288) data points was acquired from the bead in the trap at a rate of 20 kHz before each measurement series. Figure 2A shows three typical power spectra from such calibration measurements, corresponding to three different laser powers. The typical form of the response of a trapped bead according to Eq. (1), consisting of a plateau for low frequencies followed by a steep f^{-2} response for higher, is clearly visible.‡ Figure 2A shows also, however, that technical (flicker) noise appears for the lowest frequencies, which is in agreement with expectations since this type of noise has a general $f^{-\alpha}$ behavior (where $\alpha > 0$). More importantly though, Fig. 2A shows that the technical noise has been suppressed to such an extent that it only affects the measurements below 2 Hz. Vibrations of mechanical components (e.g. those of mirror and lens holders) normally appear at low frequencies, the plots show that there is virtually no influence of vibrations of optical or mechanical components in the system. Moreover, since a cut-off frequency of the technical noise of 2 Hz is considerably lower than what is the case in many other FMOT systems, (thus not optimized for long-term measurements), these curves show that the system is well adopted for long-term force

‡ A validity check of this calibration procedure has previously been performed by a comparison with the Stokes drag force and the equipartition theorem showing good agreement, thus validating the Brownian motion calibration.

measurements. For example, if the technical noise would be significant already at higher frequencies, e.g. at 20 Hz, the low frequency noise (drifts) in the system (at sub-Hz frequencies) would be correspondingly (one or two orders of magnitude) higher, thus affecting long-term measurements considerably.

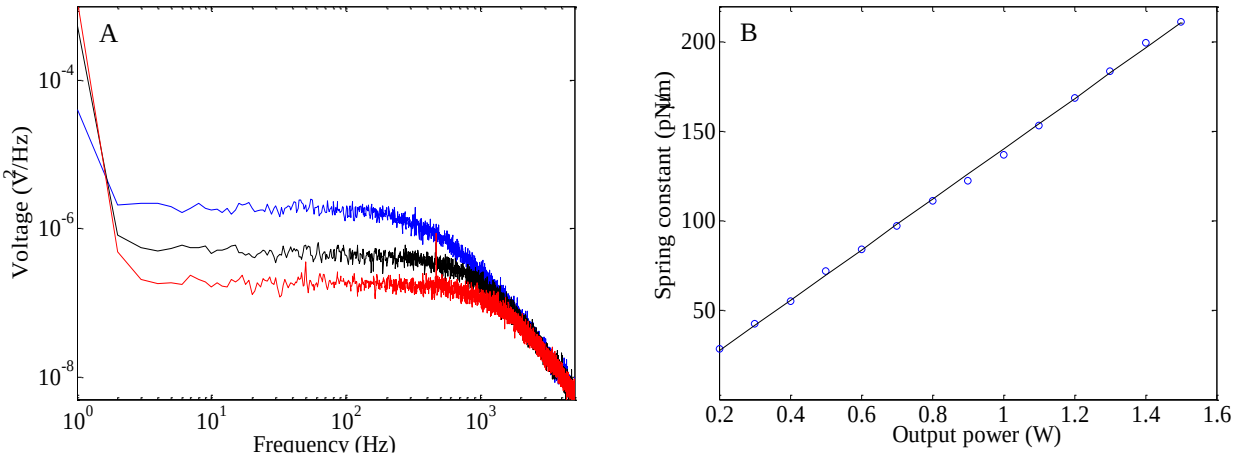

Figure 2. A) Power spectra of a trapped 3 µm bead at laser powers of 0.5 W, 1 W, and 1.5 W. Equation (1) was then fitted to each set of data, resulting in this case to trap stiffness of 67, 142, and 223 pN/µm, respectively. B) Stiffness of the trap-*vs.*-output power. The good linearity illustrates both that the system has no severe misalignments and that the Nd:YAG laser has a good intensity stability.

As a part of the optimization of the system, the stiffness of the trap is regularly measured as a function of laser power, since such a study can be indicative of possible misalignments in the system. One such curve is shown in Fig. 2B. The linearity of the curve indicates that there are no severe misalignments in the optical system.

2.3. The measurement procedure

The biological model system and the culture conditions for maintenance of the bacteria have been described previously.[23] In short, a 30 µL sample, consisting of PBS, 9.0 µm hydrophobic beads, 3.2 µm receptor coated beads, and diluted bacteria, was prepared on a coverslip.

The following measurement procedure was used for long time force spectroscopy of *E. coli* P pili. A free-floating bacterium was trapped by the optical tweezers with low power and firmly mounted on a large bead, which was immobilized to the cover slip. A small bead was subsequently trapped by the optical tweezers with normal power and brought to a position close to the bacterium. A force measuring calibration procedure, based upon Brownian motion, as described above, was used to calibrate the stiffness of the trap before each new set of measurements. The small bead, to which the pili adhere non-covalently and non-specifically, was then brought close to the bacteria and aligned. The data acquisition was started and the piezo stage was set in motion to separate the bacterium from the small bead within the equilibrium speed of unfolding/refolding, <0.1 µm/s. Since multiple pili attachments are common at small elongations, the separation was pursued until only one pilus was attached. The pilus was then extended up into region III for a complete unfolding and an overstretching of the PapA rod. The movement was then reversed, often at a force around 70-80 pN, to yield a retraction of the pilus (and a complete refolding of the PapA rod).

3. RESULTS

3.1. System characterization

The stability of the FMOT system was assessed by long-term measurements of both a free bead in the trap and a bead to which a P pilus was attached under long time (10 minutes). Panel A in Fig. 3 shows data from a free bead, whereas panel B shows the corresponding data of a bead attached to a P pilus. In this particular case, the PapA rod of the P pilus was elongated to, and held in, its unfolding region (see below), thus when the bead is exposed to the unfolding force, F_{uf} . In both cases, the data was sample with 200 Hz and filtered with 10 Hz. The figure shows, first of all, that the drift in the system is very small and that the noise from a free bead is smaller than that from a bead to which a P pilus is attached. In order to quantify the drifts and noise in the system, a 4th order polynomial, $F_{fit}(t)$, was fitted to the data. Whereas this fit provides a measure of the long term drifts of the system, the standard deviation of the difference between the measured data and the fit, $F_{meas}(t) - F_{fit}(t)$, brings information about the amount of noise. It was found that the long time fluctuations for a free bead are within 0.5 pN (over a timescale of 10 min), while the noise (given as one standard deviation, σ_F) accounts to 0.2 pN (measured over a bandwidth of 10 Hz). For the case when the bead is attached to a P pilus elongated into its unfolding state, the corresponding values for drift and noise were found to be 0.4 and 0.5 pN, respectively.

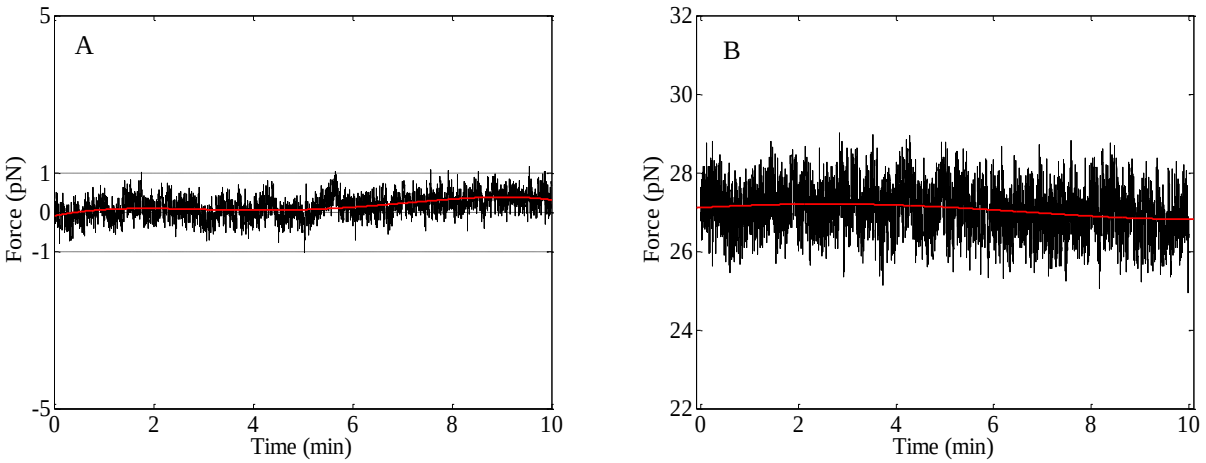

Figure 3. A) Panel shows a long-time measurement (10 min) of the response of a free bead held in the optical trap. The long termed drift in the optical tweezers is of the order of 50 fN/min and the noise originating mostly from Brownian motion is 0.2 pN. B) Panel B shows similarly made measurement of the response of a bead attached to a single P pili stretched into region II. The drift of the system is 40 fN/min whereas the standard deviation is 0.5 pN.

The low and similar values of the drift (0.5 pN for the free bead and 0.4 pN for the bead with pili attached) show, first of all, that the long-term drifts (over time scales of minutes) from the trapping and detection process in the system are only about half a pN, and secondly, that no extra drifts are introduced from the pili or the microscope table.

The difference in values of the noise (0.2 and 0.5 pN for the two cases) shows that the noise is more than twice as high in the presence of the biological model system as in comparison with a free bead. This noise can have two origins. Since the biological model system provides a direct coupling to the cover glass through the immobilized bead, it is possible that the noise originates from vibrations in the microscope. It is also possible that the increased noise originates from thermal motion of the pilus in the assay, including thermal (random) opening and closing of bonds. It is interesting to note that a random opening or closure of the outermost bond would give rise to a fluctuation of the force close to the measured value (~0.5 pN, depending on trap stiffness, length of the pili, etc).

3.2. Long-term properties of the PapA rod

In order to demonstrate the effect of repetitive unfolding and refolding cycles of the PapA rod, a series of measurements were performed in which a single P pilus was elongated and retracted throughout its entire elongation-and-retraction cycles a number of times. The panels A and B in Fig. 4 show four typical force-*vs.*-elongation and force-*vs.*-retraction curves of an individual P pilus measured in such a measurement series. Note that each consecutive curve has been shifted upwards 40 pN for display purposes.

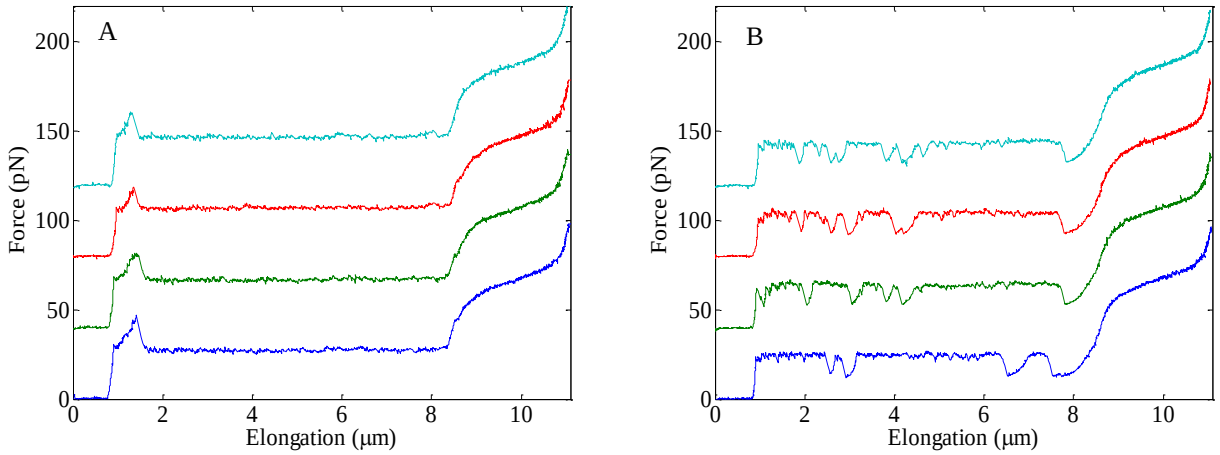

Figure 4. The unfolding of the PapA rod is not only fully reversible (the consecutive unfolding is similar to the previous one) but also possible to elongate numerous times without showing any fatigue. The panels above shows data from a series of measurement on the same pilus over a total time of >45 min. Panel A) represents data from a single pilus elongated four times in a row, whereas panel B) shows the refolding. The only difference between the unfolding/refolding is the dips, which originates from failure to refold in the absence of a nucleation kernel. A slightly lower constant level is also present in panel B.

The plots in Fig. 4A illustrate first of all the typical force-*vs.*-elongation behavior of a P pilus. As has been discussed previously in the literature,[15] the PapA rod elongates by a passage through a series of regions when exposed to mechanical stress. The first elongation region is characterized by a linear force-*vs.*-elongation response and considered to originate from an elastic stretching of the quaternary structure of the PapA rod, which in turn can be attributed to either an increase in the length of the bonds between consecutive turns of the PapA rod (the so called layer-to-layer bonds, also referred to as the n to n+3/n+4 subunit-subunit interactions in the literature[13]), by an elastic elongation of the PapA units themselves, or a combination thereof. The second region is characterized by an elongation under constant force and has been attributed to a successive opening of the layer-to-layer bonds, which gives rise to an unfolding of the quaternary structure of the PapA rod. The third region, which has an "*s*"-shape, originates from an over-stretching of the linearized PapA rod, and includes a phase transition between two discrete conformations of the linearized PapA rod. The force required for unfolding of the helix-like PapA rod under steady-state conditions has previously been assessed to 27 ± 2 pN.[15]

The typical retraction behavior, shown in Fig. 4B, is similar to that of elongation, with the only difference being some dips, which originate from a failure of the PapA rod to refold. As is investigated in a separate work, whereas the right-most dip originates from the absence of a nucleation kernel when the PapA rod is about to start to fold and therefore appears each time a PapA rod has been completely unfolded, the dips in the interior of region II result from spontaneous misfoldings and their appearance depends on, among other things, the speed of retraction. These dips are therefore not an indication of an unstable system or "fatigue" in the biological system.

In conclusion, the plots in Fig. 4 show that there is no noticeable difference between various force-*vs.*-elongation or force-*vs.*-retraction curves in a long (> 45 min) series of measurement. This shows that there are no long-time effects of

the forced unfolding and refolding of the helical structure of the PapA rod; or phrased differently, there seems not to be any effect of "fatigue" in the P pilus system. This contradicts previous results presented in the literature that has referred the elongation of the PapA rod to a "plastic" elongation.[13] These measurements instead show that the P pilus is capable of withstanding extensive cycles of strain, leading to a complete unfolding of the helical structure of its PapA rod repetitive times during the life cycle of a bacterium, without any perceptible alteration of its mechanical properties. This function is believed to be importance for bacteria in vivo since it can provide a close contact to the host cell despite repeatable urine cleaning attempts.

Figure 5, finally, shows a histogram of the distribution of unfolding forces of region II, F_{AB}, from one pilus exposed to repetitive unfolding and refoldings (~76) during one full hour, performed under equilibrium conditions. In contrast to single bond force spectroscopy,[24] which has a distribution width roughly equal to the most probable bond opening force, a significantly narrower peak (F_{AB} = 28.3 ± 0.6 pN) is obtained.[§] This can be attributed to the force clamping phenomenon that occurs when a chain molecule is elongated at a fixed speed. Since the measurements upon which Fig. 5 is based were performed under a long time (~an hour), the narrow unfolding force distribution is also an indication of the low drift in the system and the non-fatigueness of the biopolymer.

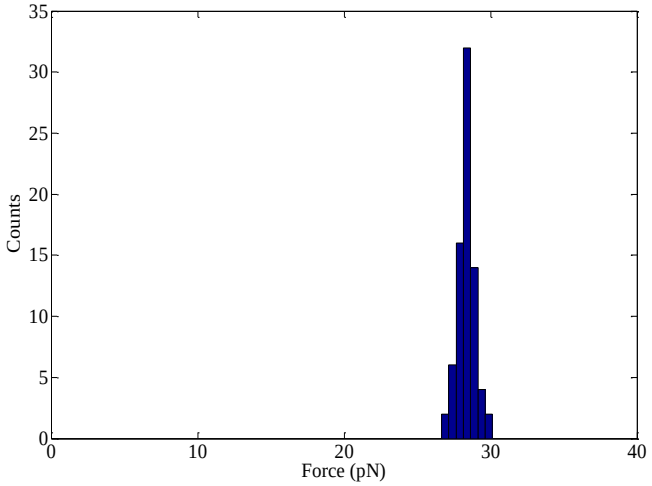

Figure 5. A histogram plot of the measured force for steady state conditions of the unfolding region F_{AB}. The narrow distribution is a result of the force clamping that takes place when the unfolding occurs in a zipper like mode and demonstrates that the drifts in the system are small under the time period of the measurement (~an hour).

4. CONCLUSION

We have presented an optical tweezers setup that is suitable for long time force measurements. The stability over long time scales has been shown and discussed. Furthermore, we have investigated the long term effects of unfolding/refolding of the PapA rod and concluded that the PapA rod is a strong, non-fatigueable biopolymer, capable of withstanding extensive strain, leading to a complete unfolding of the helical structure, repetitive times during the life cycle of a bacterium, without showing any noticeable alteration of the mechanical properties of the P pili. This function is believed to be importance for UPEC bacteria in vivo since it provides a close contact to a host cell (which is an initial step of invasion) despite repeatable urine cleaning attempts.

[§] In this particular case, an unfolding force slightly higher than what previously has been reported[15] was found. A possible explanation for this is that the unfolding rate depends on external factors, e.g. salinity and pH. This is currently under investigation.

REFERENCES

1. K. C. Neuman and S. M. Block. 2004. Optical trapping. Rev. Sci. Instr. 75:2787-2809.
2. K. Wang, J. G. Forbes, and A. J. Jin. 2001. Single molecule measurements of titin elasticity. Progress in Biophysics & Molecular Biology 77:1-44.
3. R. Merkel. 2001. Force spectroscopy on single passive biomolecules and single biomolecular bonds. Phys. Rep. 346:344-385.
4. E. Evans and K. Ritchie. 1997. Dynamic strength of molecular adhesion bonds. Biophys. J. 72:1541-1555.
5. R. Merkel, P. Nassoy, A. Leung, K. Ritchie, and E. Evans. 1999. Energy landscapes of receptor-ligand bonds explored with dynamic force spectroscopy. Nature 397:50-53.
6. M. Rief and H. Grubmuller. 2002. Force spectroscopy of single biomolecules. Chemphyschem 3:255-261.
7. J. R. Johnson and T. A. Russo. 2002. Uropathogenic Escherichia coli as agents of diverse non-urinary tract extraintestinal infections. J. Infect. Dis. 186:859-864.
8. T. A. Russo and J. R. Johnson. 2003. Medical and economic impact of extraintestinal infections due to Escherichia coli: focus on an increasingly important endemic problem. Microbes Infect. 5:449-456.
9. G. Källenius, S. B. Svenson, H. Hultberg, R. Möllby, I. Helin, B. Cedergren, and J. Winberg. 1981. Occurrence of P-fimbriated Escherichia coli in urinary tract infections. Lancet 2:1369-1372.
10. M. F. Gong and L. Makowski. 1990. Structural studies of pap pili from Escherichia coli. Biophys. J. 57:A254-A254.
11. M. F. Gong and L. Makowski. 1992. Helical structure of P pili from Escherichia coli - Evidence from X-ray fiber diffraction and scanning-transmission electron-microscopy. J. Mol. Biol. 228:735-742.
12. M. F. Gong, J. Wall, H. S. Batliwala, and L. Makowski. 1992. Structural studies of Pap adhesion pili from Escherichia coli. Faseb J. 6:A471-A471.
13. E. Bullitt and L. Makowski. 1995. Structural polymorphism of bacterial adhesion pili. Nature 373:164 -167.
14. E. Bullitt and L. Makowski. 1998. Bacterial adhesion pili are heterologous assemblies of similar subunits. Biophys. J. 74:623-632.
15. J. Jass, S. Schedin, E. Fällman, J. Ohlsson, U. Nilsson, B. E. Uhlin, and O. Axner. 2004. Physical properties of Escherichia coli P pili measured by optical tweezers. Biophys. J. 87:4271-4283.
16. E. Fällman, S. Schedin, J. Jass, B. E. Uhlin, and O. Axner. 2005. The unfolding of the P pili quaternary structure by stretching is reversible, not plastic. EMBO reports 6:52–56.
17. E. Fällman, M. Andersson, S. Schedin, J. Jass, B. E. Uhlin, and O. Axner. Dynamic properties of bacterial pili measured by optical tweezers; 2003; San Jose. Proc. SPIE. p 763-733.
18. M. Andersson, E. Fällman, B. E. Uhlin, and O. Axner. 2006. A sticky chain model of the elongation of Escherichia coli P pili under strain. Biophys. J. 90:1521-1534.
19. E. Fällman and O. Axner. 1997. Design for fully steerable dual-trap optical tweezers. Appl. Opt. 36:2107-2113.
20. K. Berg-Sorensen, L. Oddershede, E. L. Florin, and H. Flyvbjerg. 2003. Unintended filtering in a typical photodiode detection system for optical tweezers. J. Appl. Phys. 93:3167-3176.
21. S. Chu and S. J. Kron; The regents of the Stanford Leland Junior University, Stanford, California, assignee. 1992 Jan. 7. Method for optically manipulating polymer filaments. USA.
22. K. Svoboda and S. M. Block. 1994. Biological applications of optical forces. Annu. Rev. Biophys. Biomem. 23:247-285.
23. E. Fällman, S. Schedin, J. Jass, M. Andersson, B. E. Uhlin, and O. Axner. 2004. Optical tweezers based force measurement system for quantitating binding interactions: system design and application for the study of bacterial adhesion. Biosens. Bioelectron. 19:1429-1437.
24. E. Evans. 2001. Probing the relation between force - lifetime - and chemistry in single molecular bonds. Annu. Rev. Biophys. Biomem. 30:105-128.